# EQUILIBRIUM PROFILE OF ICE SHELVES

*By* T. J. O. SANDERSON

(British Antarctic Survey, Natural Environment Research Council, Madingley Road, Cambridge CB3 0ET, England)

ABSTRACT. Using expressions for ice-shelf creep derived by Weertman (1957) and Thomas (1973[b]) a general method is developed for calculating equilibrium thickness profiles, velocities, and strain-rates for any ice shelf. This is done first for an unconfined glacier tongue and the result agrees well with data for Erebus Glacier tongue (Holdsworth, 1974). Anomalies occur within the first 3 km after the hinge zone and these are too great to be the result of local bottom freezing; they are probably due to disturbance of the velocity field. Secondly, profiles are calculated for bay ice shelves. Thickness gradients are largely independent of melt-rate or flow parameters but are inversely proportional to the width of the bay. Data from Antarctic ice shelves agree with this result both qualitatively and quantitatively. The theory is readily extended to ice shelves in diverging and converging bays. An ice shelf in a diverging bay can only remain intact if it is thick enough and slow enough to creep sufficiently rapidly in the transverse direction. If it cannot, it will develop major rifts or will come adrift from the bay walls. It is then likely to break up. The presence of ice rises or areas of grounding towards the seaward margin can radically alter the size of the ice shelf which can form. The theory could be used as a starting point to study non-equilibrium behaviour.

RÉSUMÉ. *Profil d'équilibre d'une calotte glaciaire.* A partir des expressions du glissement des calottes glaciaires données par Weertman (1957) et Thomas (1973[b]), on développe une méthode générale pour calculer les profils d'équilibre en épaisseur, les vitesses et les déformations d'une calotte glaciaire. On le fait d'abord pour une langue de glace de versant et les résultats concordent bien avec les mesures sur la langue flottante de l'Erebus Glacier (Holdsworth, 1974). Des anomalies apparaissent dans les trois premiers kilomètres après la zone charnière et elles sont trop importantes pour être le résultat d'un gel localisé au fond; elles sont probablement dues à des troubles dans le champ des vitesses. En second lieu, on a calculé des profils pour les glaces de baies. Les gradients d'épaisseur sont largement indépendants des vitesses de fusion ou des paramètres d'écoulement mais sont inversement proportionnels à la largeur de la baie. Les données issues des calottes antarctiques corroborent bien ces résultats, qualitativement et quantitativement. La théorie est facile à étendre aux glaces recouvrant des baies divergentes ou convergentes. Une couverture glaciaire dans une baie divergente ne peut rester intacte qui si elle est assez épaisse et assez lente pour glisser assez vite dans la direction transversale. Si elle ne le peut, elle va développer de profondes crevasses ou viendra divaguer le long des flancs de la baie. Elle a alors toutes les chances de se briser. La présence de dômes insulaires de glace ou de zones déglacées à proximité du littoral peut altérer radicalement la dimension des calottes qui peuvent se former. On pourrait utiliser la théorie comme point de départ et pour l'étude du comportement loin de l'état d'équilibre.

ZUSAMMENFASSUNG. *Das Gleichgewichtsprofil von Schelfeisen.* Mit Hilfe der von Weertman (1957) und Thomas (1973[b]) hergeleiteten Formeln für das Kriechen von Schelfeisen wird eine allgemeine Methode zur Berechnung von Gleichgewichtsprofilen, Geschwindigkeiten und Verformungsraten für ein beliebiges Schelfeis entwickelt. Dies geschieht zunächst für eine unbegrenzte Gletscherzunge; das Ergebnis stimmt gut mit Daten für die Zunge des Erebus Glaciers überein (Holdsworth, 1974). Abweichungen treten innerhalb der ersten 3 km nach der Ablösungszone auf; sie sind zu gross, als dass sie die Folge lokalen Auffrierens an der Unterseite sein könnten. Vermutlich beruhen sie auf Störungen im Geschwindigkeitsfeld. Sodann werden Profile für Bucht-Schelfeise berechnet. Die Dickengradienten sind weitgehend unabhängig von der Abschmelzrate oder von Fliessparametern, jedoch umgekehrt proportional zur Breite der Bucht. Daten von antarktischen Schelfeisen stimmen mit diesem Ergebnis sowohl qualitativ wie quantitativ überein. Die Theorie lässt sich leicht auf Schelfeise in divergierenden und konvergierenden Buchten erweitern. Ein Schelfeis in einer divergierenden Bucht kann nur dann intakt bleiben, wenn es dick und langsam genug ist, um schnell genug in Querrichtung kriechen zu können. Trifft dies nicht zu, so wird es grössere Pressrücken entwickeln oder sich von den Küsten der Bucht ablösen. Es dürfte dann zusammenbrechen. Das Vorhandensein von Eiskuppeln oder Aufsetzgebieten gegen den vorderen Rand hin kann die Grösse des entstehundsfähigen Schelfeises grundlegend ändern. Die Theorie könnte den Ausgangspunkt für das Studium nichtstationären Verhaltens bilden.

## I. INTRODUCTION

The Antarctic continent is surrounded by large expanses of floating ice shelf, some of it flowing freely out to sea, some of it confined in bays or restricted by islands and areas of grounding. Such ice shelves are fed by the inland ice sheet or by valley glaciers, and as they move out to sea they are subject to creep under their own weight, drag at their sides, snow accumulation on the upper surface, and melting or freezing at the bottom surface; the shape they assume is therefore the result of a delicate balance of forces. Most ice shelves have been

435

in existence for many thousands of years and, if climatic and input conditions have not varied significantly, they may be expected to have reached a state of dynamic equilibrium. By setting up equations of balance we shall describe this state and calculate expected thickness profiles, velocities, and strain-rates.

There is reason to believe that many ice shelves are not in a state of equilibrium (Budd, 1966; Hughes, 1977; Thomas, 1976; Bishop and Walton, unpublished report). Nonetheless, a study of the expected equilibrium state is an essential starting point for any study of non-equilibrium behaviour. Here we shall concern ourselves only with equilibrium behaviour, first for an unconfined ice shelf or glacier tongue, and secondly for an ice shelf within a bay or bounded by areas of grounding.

Barkov (1970) has described how an unconfined ice shelf subject to positive net accumulation should approach an equilibrium thickness as it flows out to sea. At a large distance from the shore, a balance is reached between thickening due to accumulation and thinning due to creep. In the study reported here a more general approach allows bottom melting in the formulation of the equations, and examines equilibrium behaviour over the entire length of the ice shelf, not just its asymptotic behaviour.

## II. EQUILIBRIUM PROFILE OF AN UNCONFINED ICE SHELF

### General theory

Consider a laterally unconfined ice shelf or glacier tongue with axes as shown in Figure 1. The $x$ and $y$ axes are horizontal at sea-level and $z$ is measured vertically. The ice shelf flows out to sea in the positive $x$ direction and its thickness $H$ and velocity $u$ vary slowly over its length. The height of the upper surface above sea-level is denoted by $h$.
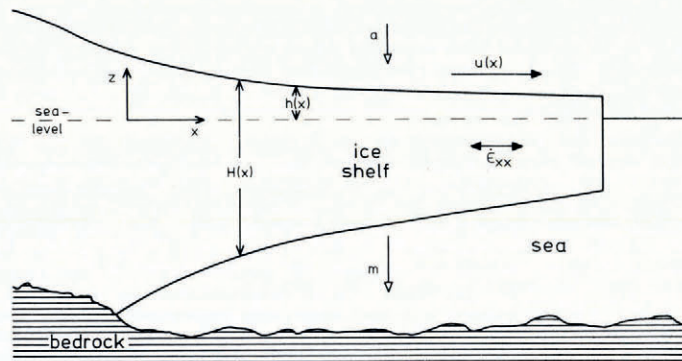


Fig. 1. Longitudinal section of an ice shelf.

To describe the deformation processes taking place within the ice mass we shall use the strain-rates $\dot{\epsilon}_{ij}$ and the stresses $\sigma_{ij}$ $(i, j = x, y, z)$, and we shall assume these to be related by the flow law for polycrystalline ice (Paterson, 1969, p. 82):

$$\dot{\epsilon} = (\tau/B)^n$$

where $\dot{\epsilon}$ and $\tau$ are defined through the second invariants of the strain-rate and stress-deviator tensors,

$$2\dot{\epsilon}^2 = \dot{\epsilon}_{ij}\dot{\epsilon}_{ij}$$

and

$$2\tau^2 = \sigma_{ij}{}'\sigma_{ij}{}',$$

with stress deviators $\sigma_{ij}'$ defined by

$$\sigma_{xx}' = \sigma_{xx} - \tfrac{1}{3}\sigma_{ii}, \quad \text{etc.}$$

and

$$\sigma_{xy}' = \sigma_{xy}, \quad\quad \text{etc.}$$

The parameter $B$ is dependent on temperature and may therefore be expected to vary with depth in the ice shelf. Thomas (1973[a]) found that $n$ is about three for Antarctic ice shelves; this is also the value expected if creep processes are controlled by dislocation glide.

For an unconfined ice shelf there is complete symmetry for all stresses and strain-rates in the $x$ and $y$ directions, at least along the centre line, so that horizontal shear quantities are zero. Where the thickness changes slowly, vertical shear quantities are also negligible (Sanderson and Doake, 1979).

In order to find the equilibrium profile we propose to repeat for ice shelves the exercise Nye (1959) carried out for ice caps, that is, to find expressions for velocity and strain-rate as functions of distance $x$ and thickness $H$, apply a steady-state requirement, and then solve the equations to determine the resulting profile.

Velocities and strain-rates may be found by considering the analysis given by Weertman (1957). We consider the static equilibrium of stresses acting on any vertical element far from the ice front, and require that the total force within the ice shelf acting on any vertical column must balance the total force exerted by sea-water pressure. If the density of sea-water is $\rho_w$ this means that

$$\int_b^s \sigma_{xx}\,\mathrm{d}z = \int_b^0 \rho_w g(H-h-z)\,\mathrm{d}z$$

where $s$ and $b$ refer to the upper and lower surfaces of the ice shelf. For a variable ice-shelf density $\rho(z)$ this leads to

$$\tau = \frac{g}{\sqrt{3}H}\left\{\int_b^s \int_z^s \rho(z)\,\mathrm{d}z\,\mathrm{d}z - \frac{1}{2}\rho_w(H-h)^2\right\},$$

and therefore

$$\dot\epsilon_{xx} = \frac{1}{\sqrt{3}}\left[\frac{g}{\sqrt{3}H\bar{B}}\left\{\int_b^s \int_z^s \rho(z)\,\mathrm{d}z\,\mathrm{d}z - \frac{1}{2}\rho_w(H-h)^2\right\}\right]^n \tag{1}$$

where

$$\bar{B} = \frac{1}{H}\int_b^s B(z)\,\mathrm{d}z,$$

the average of $B$ over depth.

If we know, or can model, the functions $B(z)$ and $\rho(z)$, then Equation (1) gives $\dot\epsilon_{xx}$ as a function only of thickness $H$. For clarity, let

$$\dot\epsilon_{xx} = f(H). \tag{2}$$

Now, the velocity of the ice shelf may be written as

$$u(x) = u(0) + \int_0^x \dot\epsilon_{xx}\,\mathrm{d}x$$

where $u(0)$ is the velocity at some chosen point of origin, for instance the hinge zone. This may be written as

$$u(x) = u(0) + \int_0^x f(H) \, dx, \tag{3}$$

so that we now have velocity and strain-rate in terms only of $x$ and $H$. We now consider the condition for steady state. If the ice shelf undergoes accumulation rate $a$ and melt rate $m$ (positive for melting), then the condition for steady state may be found by considering a moving, deforming column of ice. Thickness gradients in the $y$ direction are negligible so that the continuity equation is

$$\rho_i(a-m) - \bar{\rho}(\dot{\epsilon}_{xx} + \dot{\epsilon}_{yy}) H - \bar{\rho}u \frac{\partial H}{\partial x} = 0 \tag{4}$$

where $a$ and $m$ are expressed in metres of pure ice per unit time, $\rho_i$ is the density of pure ice, and

$$\bar{\rho} = \frac{1}{H} \int_b^s \rho(z) \, dz,$$

the average density through the ice shelf.

Now, by symmetry $\dot{\epsilon}_{xx} = \dot{\epsilon}_{yy}$, and substituting Equations (2) and (3) into Equation (4) and re-arranging we have a differential–integral equation solely in terms of $x$ and $H$,

$$\frac{\partial H}{\partial x} = \{(\rho_1(a-m)/\bar{\rho}) - 2f(H) H\} \Big/ \left\{ u(0) + \int_0^x f(H) \, dx \right\}. \tag{5}$$

This equation cannot be solved analytically, but in principle it gives thickness as a function of distance; it enables an equilibrium profile to be calculated. It is most readily solved numerically by tracing the course of the curve using small steps, for, if we take some values of $H(0)$ and $u(0)$ at a starting point, we can calculate the slope $\partial H/\partial x$ by Equation (5) and hence can calculate the increment $\delta H$ for some appropriately small interval $\delta x$. We can then carry out the same process for our new point $H(\delta x)$, $u(\delta x)$, and so on to the values at the $r$th step, $H_r$ and $u_r$. In such a process of finite steps we have to calculate the integral term in the denominator as a finite sum; for the $r$th step

$$\int_0^x f(H) \, dx \approx \sum_0^r f(H_r) \, \delta x,$$

and as we make each further step we add the increment

$$f(H_{r+1}) \, \delta x.$$

The full expression for the increment in passing from one step to another is, in the limit of small intervals,

$$\delta H = \cfrac{\cfrac{\rho_i(a-m)}{\bar{\rho}} - \cfrac{2H}{\sqrt{3}} \left[ \cfrac{g}{\sqrt{3}H\bar{B}} \left\{ \int_b^s \int_z^s \rho(z) \, dz \, dz - \frac{1}{2} \rho_w (H-h)^2 \right\} \right]^n}{u(0) + \cfrac{1}{\sqrt{3}} \int_0^x \left[ \cfrac{g}{\sqrt{3}H\bar{B}} \left\{ \int_b^s \int_z^s \rho(z) \, dz \, dz - \frac{1}{2} \rho_w (H-h)^2 \right\} \right]^n dx} \, \delta x. \tag{6}$$

Before we can use this, we shall need to consider the form of the density integrals within the equation.

*Density–depth relationship*

Thomas (1973[a]) noted that we should not be tempted to assume that density is constant through an ice shelf. Such an assumption leads to an overestimate of $\tau$ by a factor of about two and therefore an overestimate of $\dot{\epsilon}$ by a factor of about eight.

Schytt (1958) has considered different ways of modelling the variation of snow density with depth. Using data gathered at Maudheim he first fits a simple decaying exponential

$$\rho(z) = \rho_i - d \exp\{-b(h-z)\} \tag{7}$$

where $d$ and $b$ are empirical constants, and then goes on to provide two other possible functions which both follow the Robin suggestion for a more realistic model of the processes controlling densification (Robin, 1958, p. 92) where "the proportional change in air space in firn is in linear proportion to the change in stress due to the weight of material above a given level". This assumption leads to a model of the form

$$\rho(z) = \frac{\rho_i \beta \exp\{-\gamma(h-z)\}}{1 + \beta \exp\{-\gamma(h-z)\}} \tag{8}$$

where $\beta$ and $\gamma$ are empirical constants.

Schytt (1958, p. 124) compares these models with field data. All three models must be considered to give adequate agreement in view of the wide scatter of the data. In evaluating the double integrals in Equation (6) it is found that Equation (7) is integrable while Equation (8) is not. We shall therefore follow Thomas (1973[a]) in adopting Equation (7) with constants fitted appropriately.

How should the constants $b$ and $d$ be fitted? The constant $d$ is readily related to the average density of surface snow $\rho(h)$, which we may assume to remain constant along the ice shelf. We have

$$\rho(h) = \rho_i - d.$$

$b$ is less easy to fit. Schytt found a value for $b$ of 0.025 8 m$^{-1}$ at Maudheim, for an ice-shelf thickness of about 200 m. This value implies that the average density through the ice shelf is 0.827 Mg m$^{-3}$. In extrapolating Schytt's results to other ice shelves we therefore have two alternatives: either we assume that the attenuation factor $b$ remains constant as thickness varies, in which case the average density of the ice shelf must vary, or we assume that the average density of the ice shelf remains constant as thickness varies, in which case $b$ must vary. Studies on Erebus Glacier tongue (Holdsworth, 1974) showed no systematic variation of average density while the thickness varied by a factor of two, and we shall therefore assume average density to be constant. I have found that trial calculations using the alternative assumption do not lead to radically different profiles.

Let us require then that the ice-shelf density be a constant, $\bar{\rho}$; thus,

$$\frac{1}{H} \int_b^s \rho(z)\,\mathrm{d}z = \bar{\rho},$$

and on performing the integration in Equation (7) we find that

$$(d/b)/(1 - \exp(-bH)) = H(\rho_i - \bar{\rho}),$$

which we wish to solve for $b$ as a function of $H$. An exact solution cannot be given analytically, but a simplification can be made if we consider the magnitude of $\exp(-bH)$. Schytt (1958) quotes a value of $b = 0.025\ 8$ m$^{-1}$ for Maudheim, with $H \approx 200$ m, so $\exp(-bH) \approx 0.006$ and is negligible. We can therefore write

$$b = \frac{d}{H(\rho_i - \bar{\rho})}.$$

Now consider the double integral in Equation (6). Using Equation (7) it becomes

$$\int_b^s \int_z^s \rho(z) \, \mathrm{d}z \, \mathrm{d}z = \frac{\rho_i H^2}{2} + \frac{d}{b^2} \{1 - \exp(-bH) - bH\}$$

$$\approx \left\{ \frac{\rho_i}{2} + \frac{(\rho_i - \bar{\rho})}{d} (\rho_i - \bar{\rho} - d) \right\} H^2,$$

using our approximation. We find then that Equation (6) becomes, after substitution and simplification,

$$\delta H = \frac{\rho_i(a-m)/\bar{\rho} - 2CH^{n+1}}{u(0) + \int_0^x CH^n \, \mathrm{d}x} \delta x,$$

with $C$ defined through

$$\dot{\epsilon}_{xx} = CH^n = \frac{1}{\sqrt{3}} \left[ \frac{g}{B\sqrt{3}} \left\{ \frac{(\bar{\rho} - \rho_i)^2}{d} + \bar{\rho} - \frac{\rho_i}{2} - \frac{\bar{\rho}^2}{2\rho_w} \right\} \right]^n H^n. \tag{9}$$

We shall now examine how well this formula agrees with experimental data.


*Agreement with reality*

The Erebus Glacier tongue, McMurdo Sound, Antarctica, has been examined in some detail by Holdsworth (1974). It extends 12 km into the Ross Sea, is about 1 500 m wide, and is between 120 and 360 m in thickness. It is believed to be floating freely. Using a variety of data sources Holdsworth determined thicknesses, velocities, and strain-rates along the ice tongue and used these to calculate melt-rates after making the assumption of steady state and taking a value for the flow-law parameter $\bar{B}$. In using these values to calculate an equilibrium profile we are therefore using a circular argument; however, the calculation of the profile does at least demonstrate whether the values found are internally consistent and give the expected behaviour between data points. We shall also see that it provides some information on behaviour in the vicinity of the hinge zone.

Holdsworth gives the following values:

$$\bar{B} = 1 \times 10^8 \text{ N m}^{-2} \text{ s}^{\frac{1}{3}},$$
$$(m-a) = 1.2 \text{ m a}^{-1} \text{ (ice)},$$
$$\bar{\rho} = 0.867 \text{ Mg m}^{-3}.$$

We take

$$\rho_w = 1.028 \text{ Mg m}^{-3},$$

and

$$\rho_i = 0.917 \text{ Mg m}^{-3}.$$

We have adjusted $d$ so that Equation (7) gives a density of about 0.60 Mg m$^{-3}$ at a depth of 10 m. This accords with density measurements made by Stuart and Bull (1963) on the nearby Ross Ice Shelf. We find that $d$ has the value 0.41 Mg m$^{-3}$.

We must choose a starting point in order to calculate an equilibrium profile. First, we try fitting to data at the hinge zone. Extrapolating Holdsworth's data we take the values

$$H(0) = 370 \text{ m} \quad \text{and} \quad u(0) = 102.5 \text{ m a}^{-1}.$$

The resulting profile, found by taking incremental steps 25 m long in the $x$ direction, is shown in Figure 2. It shows poor agreement in that it thins too rapidly. We therefore try starting at alternative points which are 1, 2, and 3 km from the hinge zone. For starting
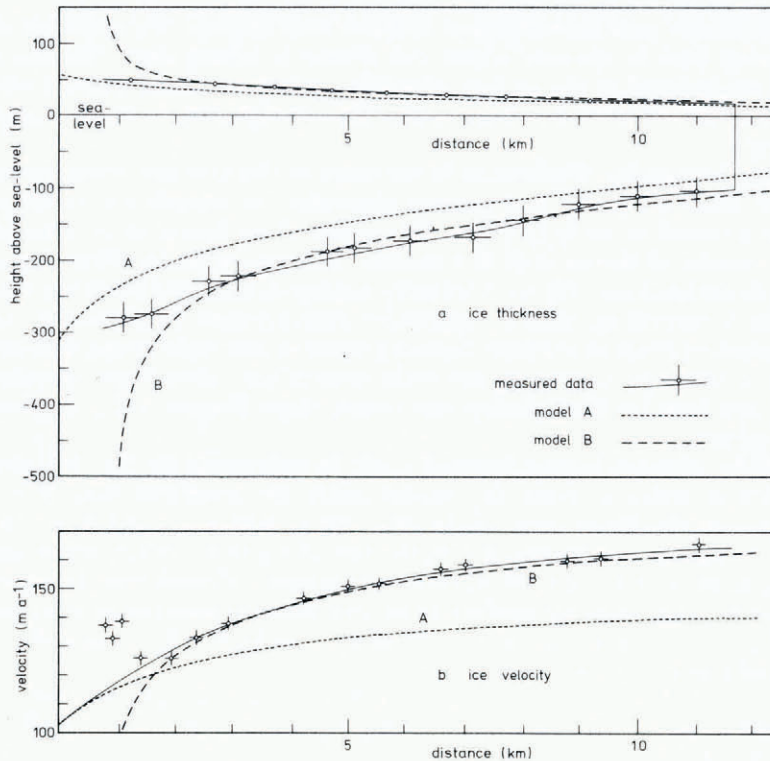
*Fig. 2. Comparison of models with (a) ice thicknesses and (b) ice velocities measured by Holdsworth (1974) for Erebus Glacier tongue. The solid line shows Holdsworth's assumed fit to his data points. The dashed lines show model A, in which the model is fitted to data at the hinge zone, and model B, in which the model is fitted to data at the 3 km mark.*

points near the hinge zone, agreement is still poor but it is found that starting points further than about 3 km from the hinge zone all give acceptable agreement. At 3 km we take

$$H(0) = 272 \text{ m} \quad \text{and} \quad u(0) = 137.5 \text{ m a}^{-1},$$

and we compute the profile by working both forward and backward from the 3 km mark. Figure 2 shows that the agreement here is very good from the 3 km mark onwards, both in thickness profile and in velocity. Any discrepancies fall well within the error bars of the measured values. This shows that the model is essentially correct and that the measured data and calculated parameters are internally consistent over the greater part of the glacier tongue.

### Behaviour near the hinge zone

At distances less than 3 km from the hinge zone our model departs from the measured data. We find that the ice shelf has to thicken very rapidly towards the hinge zone and its velocity falls dramatically. At about 0.75 km from the hinge zone the model breaks down completely, giving an infinite thickness and zero velocity. This discrepancy must in some way be connected with the process of transition between a land glacier and a floating ice shelf, a process which is not at present adequately understood. There are two principal changes taking place during this transition. First, the velocity distribution through the ice must change from the form characteristic of a land-based glacier (in which velocities decrease from the surface downwards becoming zero at the ice–bedrock interface) to that characteristic of an ice shelf (in which

negligible shear occurs and the velocity is uniform with depth). We expect a complicated stress and velocity field in the area where this change is taking place (Holdsworth, 1977). Secondly, the temperature at the bottom generally undergoes a large change when it comes into contact with sea-water rather than rock. This change may well be accompanied by bottom freezing.

If the change in velocity distribution is the cause of the anomaly, then our model gives us information about its extent and general character. It extends for about 3 km which corresponds to a period of 20 to 25 years. We expect these figures to be dependent on the thickness and velocity of the ice shelf in question. The nature of the effect seems to be that as ice flows from the land into the sea it initially undergoes less rapid thinning than would be expected. This is surprising, since a qualitative consideration (Holdsworth, 1977) of the velocity field involved leads us to expect thinning which is *more* rapid as the slow-moving basal ice accelerates to the same velocity as the main body of ice. Data from Maudheim Is-shelf (Robin, 1958) and Ross Ice Shelf (Robin and others, 1970; Hughes, 1975) appear to confirm Holdsworth's picture.

Let us consider whether bottom freezing could be responsible for the thickness anomaly. It is found that in order to make the model satisfy the condition that $H = 370$ m and $u = 102.5$ m a$^{-1}$ at the hinge zone while $H = 272$ m and $u = 137.5$ m a$^{-1}$ at the 3 km point we have to assume bottom freezing at the rate of 3.0 m a$^{-1}$ of ice, which amounts to a total accretion of some 75 m over the distance in question. Considering that oceanographic conditions near the hinge zone are unlikely to be very different from conditions over the rest of the glacier tongue, we must account for the freezing by looking to the source of cold provided by the cold land glacier as it becomes afloat.

Robin (1955) calculates the temperature $T(z)$ through a land-based ice sheet as a function of accumulation $a$, surface temperature $T_s$, and constant temperature gradient $(\partial T/\partial z)_b$ at the base. His formula is

$$T(z) = T_s + \left(\frac{\pi k H}{2a}\right)^{\frac{1}{2}}\left(\frac{\partial T}{\partial z}\right)_b \left[\mathrm{erf}\left(\frac{2kH}{a}\right)^{-\frac{1}{2}}\xi - \mathrm{erf}\left(\frac{2kH}{a}\right)^{-\frac{1}{2}}H\right]$$

where $\xi = z - H + h$, the height above the bottom of the ice shelf, and $k$ is the thermal diffusivity. We have used

$$\mathrm{erf}\, x = \frac{2}{\sqrt{\pi}}\int_0^x \exp\left(-\Upsilon^2\right)\mathrm{d}\Upsilon.$$

Let us take the average inland accumulation rate to be 0.2 m a$^{-1}$ (Stuart and Bull, 1963). We take

$$H = 350 \text{ m},$$
$$T_s = -19.5°\text{C (Holdsworth, 1974)},$$
$$k = 1.18 \times 10^{-6} \text{ m}^2 \text{ s}^{-1},$$

and

$$(\partial T/\partial z)_b = -0.023 \text{ deg m}^{-1} \text{ (Robin, 1955)}.$$

The resulting temperature profile is shown in Figure 3. In calculating temperature changes we shall be interested in the temperature profile near the bottom of the ice shelf. This portion is so close to linear that, for the purposes of the calculations here, we shall treat it as a straight line, as shown by the dashed line. The temperature at the base is $-13.4°$C and the gradient is $-0.023$ deg m$^{-1}$. Now, in order to calculate the maximum amount of water freezing which could be caused by placing this cold base in sea-water we need to calculate the way in which temperature change is transmitted through the ice shelf. Consider a simple, constant-thickness conduction model in which the temperature at the base is suddenly altered from
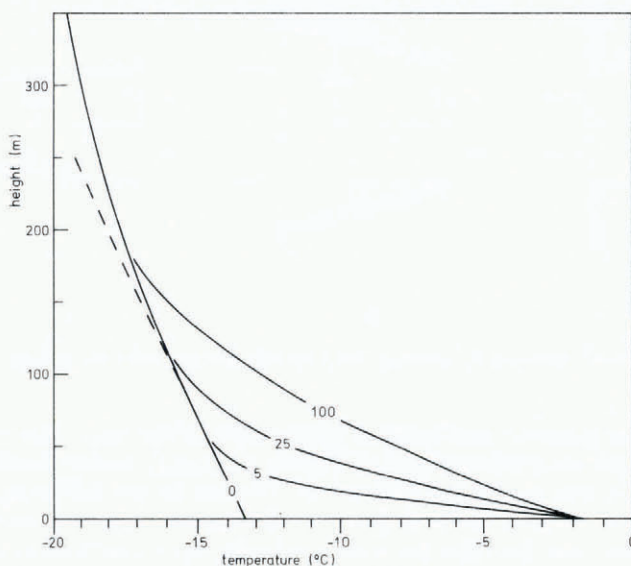
Fig. 3. *Simple model of temperature changes as a land-based glacier becomes afloat. The solid lines show the temperature profiles after 0, 5, 25, and 100 years, plotted against height ξ above the bottom of the ice shelf. The dashed line shows the linear initial profile used to simplify the conduction calculation.*

−13.4°C to −1.8°C, the temperature of the ice equilibrium with typical Antarctic sea-water (Wexler, 1960). Carslaw and Jaeger (1959, p. 99) treat this general problem, and for our particular case their formula reduces to:

$$T(z) = T_\text{b} + (T_\text{s}{}' - T_\text{b})\frac{\xi}{H} + 2\sum_{n=1}^{\infty}\frac{T_0 - T_\text{b}}{n\pi}\sin\left(\frac{n\pi\xi}{H}\right)\exp\left(\frac{-kn^2\pi^2 t}{H^2}\right)$$

where $T_0 = -13.4°C$, $T_\text{b} = -1.8°C$, and $T_\text{s}{}' = -21.5°C$, the extrapolated surface temperature for our linear model. Figure 3 shows the temperature profiles for the first 100 years. Looking at the temperature profile after 25 years, which is the time taken to reach the 3 km point, we see that the bottom 75 m of the ice shelf has undergone an average temperature rise of about 6 deg. The heat capacity of ice is 2.09 kJ kg⁻¹ deg⁻¹ (Hobbs, 1974, p. 362), so that this warming requires $8.15 \times 10^5$ kJ of heat per unit area of ice shelf. Making the extreme assumption that all this heat is supplied through the freezing of sea-water onto the base we find, taking the latent heat of fusion of ice to be 333.6 kJ kg⁻¹ (Hobbs, 1974, p. 361), that it would result in the freezing of 2.7 m of ice over the total period of 25 years. This amounts to an average of only 0.11 m a⁻¹, though we expect the freezing to be more intense at the hinge line. This amount, which may be an overestimate, is not nearly large enough to account for the anomaly in the thickness profile. Unless some other effect is causing intense freezing near the hinge zone we must therefore conclude that the thickness anomaly is a result of changes in the velocity field.

## III. EQUILIBRIUM PROFILE OF A BAY ICE SHELF

### (i) *General theory*

Consider an ice shelf confined on two sides by parallel, vertical rock faces and flowing out to sea in the positive $x$ direction (Fig. 4a). This is the model treated by Thomas (1973[b]). To derive an expression for the strain-rate at a point on the ice shelf we consider the combined
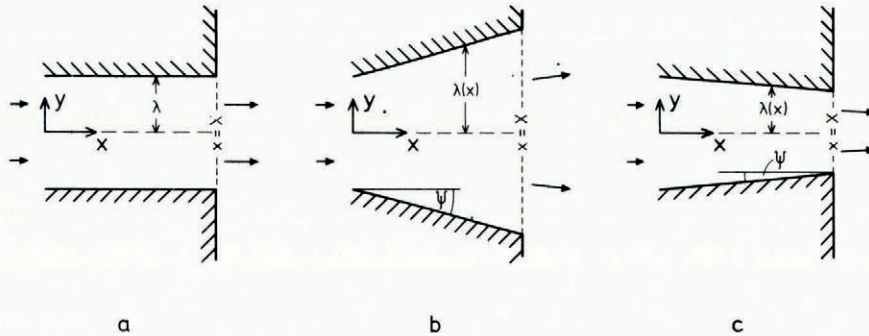
a       b       c

*Fig. 4. Plan views of ice shelves in (a) a parallel-sided bay, (b) a bay with diverging sides, and (c) a bay with converging sides.*

forces due to sea-water pressure and to shear at the sides of the bay. The sea-water force is the same as in the simple unconfined model of Weertman (1957) used in Section II. A reasonable form for the force due to shear is derived by Thomas in the following way: The force per unit volume due to shear stress acting on an element at $(x, y, z)$ is given by $-\partial\sigma_{xy}/\partial y$ at the point in question, and therefore the total up-stream force due to shear along the section between $x = x$ and $x = X$ acting on a vertical element of unit width in the $y$ direction is

$$F_s = -\int_x^X \int_b^s \frac{\partial\sigma_{xy}}{\partial y}\, \mathrm{d}z\, \mathrm{d}x. \tag{10}$$

The line $x = X$ represents the limit of the influence of the bay sides on the ice shelf. Beyond this line the ice shelf can be considered to be unconfined.

Thomas makes two further assumptions:

(i) that $\partial\sigma_{xy}/\partial y$ is a constant across the ice shelf in the $y$ direction, so that shear stress varies linearly. Shear stress is therefore given by

$$\sigma_{xy} = y\, \frac{\partial\sigma_{xy}}{\partial y}, \tag{11}$$

since it is zero along the centre line by symmetry considerations;

(ii) that shear stress at the sides, averaged over $z$, reaches some limiting value $\bar\tau_s$, independent of $x$. We expect $\bar\tau_s$ to be of the order of 1 bar, although recent work (Hughes, 1977) has suggested that it may fall to 0.4 bar if preferred crystal orientations are established by fast-moving ice. If $\lambda$ is the half-width of the ice shelf then by Equation (11) we have at the sides

$$\sigma_{xy} = \bar\tau_s = \lambda\, \frac{\partial\sigma_{xy}}{\partial y},$$

so that

$$\frac{\partial\sigma_{xy}}{\partial y} = \frac{\bar\tau_s}{\lambda}.$$

We can therefore write

$$\int_b^s \frac{\partial\sigma_{xy}}{\partial y}\, \mathrm{d}z = \frac{\bar\tau_s H}{\lambda},$$

and Equation (10) becomes:

$$F_s = -\int_x^X \frac{\bar{\tau}_s H}{\lambda} \, dx.$$

Now, Thomas's general expression for the strain-rate in an ice shelf may be written

$$\dot{\epsilon}_{xx} = \frac{\theta}{(\bar{B}H)^n} \left\{ g \int_b^s \int_z^s \rho_i(z) \, dz \, dz - F \right\}^n \tag{12}$$

where

$$F = -\int_b^s \sigma_{xx} \, dz$$

and is the total force due to sea-water pressure and shear which opposes the movement of a unit vertical section of ice shelf. $\theta$ is a number which takes account of the relative contributions of shear and longitudinal stresses to the effective stress term in the flow law; if $\alpha$ and $\beta$ are defined through $\dot{\epsilon}_{yy} = \alpha \dot{\epsilon}_{xx}$ and $\dot{\epsilon}_{xy} = \beta \dot{\epsilon}_{xx}$ then $\theta$ may be expressed as

$$\theta = \frac{(1 + \alpha + \alpha^2 + \beta^2)^{(n-1)/2}}{(2 + \alpha)^n}. \tag{13}$$

For a bay with parallel sides there is no component of velocity in the $y$ direction, and hence $\dot{\epsilon}_{yy} = 0$ and $\alpha = 0$. Further, along the centre line $\dot{\epsilon}_{xy} = 0$, so that $\beta = 0$; therefore $\theta = 2^{-n}$. On the centre line of a bay ice shelf the strain-rate is then given by

$$\dot{\epsilon}_{xx} = \left[ \frac{g}{2\bar{B}H} \left\{ \int_b^s \int_z^s \rho_i(z) \, dz \, dz - \tfrac{1}{2} \rho_w (H-h)^2 \right\} + \frac{\bar{\tau}_s}{2\bar{B}H} \int_x^X \frac{H}{\lambda} \, dx \right]^n. \tag{14}$$

Our earlier formula, Equation (1), for strain-rates in a glacier tongue gave $\dot{\epsilon}_{xx}$ as a function only of thickness $H$; Equation (14) for a bay ice shelf gives $\dot{\epsilon}_{xx}$ as a function of thickness $H$ and horizontal distance $(X-x)$ from the ice front. In calculating the steady-state profile of an ice shelf we therefore need to set up boundary conditions at the ice front and integrate backwards towards the hinge zone. We cannot start at the hinge zone, since we should then need to know in advance the form of thickness over the whole distance between the hinge zone and the ice front—this is what we are trying to calculate.

For the case of an ice shelf restricted by parallel sides we have the condition that $\dot{\epsilon}_{yy} = 0$, and hence the condition for steady state, Equation (4), becomes

$$\frac{\rho_i(a-m)}{\bar{\rho}} - \dot{\epsilon}_{xx}H - u \frac{\partial H}{\partial x} = 0,$$

for the centre line of the ice shelf.

If the velocity of the ice shelf at $x = X$ is $u(X)$ then we can calculate increments of height in the negative $x$ direction through the formula

$$\delta H = \frac{\rho_i(a-m)/\bar{\rho} - H\dot{\epsilon}_{xx}}{u(X) + \int_X^x \dot{\epsilon}_{xx} \, dx} \, \delta x, \tag{15}$$

where

$$\dot{\epsilon}_{xx} = \left\{ \frac{gH}{2\bar{B}} \left( \frac{(\rho_1-\bar{\rho})^2}{d} - \frac{\rho_1}{2} + \bar{\rho} - \frac{\bar{\rho}^2}{2\rho_w} \right) + \frac{\bar{\tau}_s}{2\bar{B}H} \int_x^x \frac{H}{\lambda} \, dx \right\}^n, \qquad (16)$$

with the assumption, as in Section II, that the mean density of the ice shelf is constant along its length.

In constructing the best possible model for a particular ice shelf we should consider all data available for such parameters as accumulation and melt, mean density, and mean temperature, and we should examine the way in which these vary along the length of the ice shelf. If the ice shelf does not have parallel boundaries we should take account of any transverse strain-rates due to the divergence of flow lines (Robin, 1958, p. 121). Initially we look at an ice shelf for which all these parameters are constant.

The ice shelf forms in a rectangular bay of width $2\lambda$ and length $L$. It is fed by a glacier at its landward margin, is subject to melt and accumulation, and discharges freely into the sea once it has escaped the influence of the bay. We have to choose the boundary conditions $H(X)$ and $u(X)$ at the seaward margin of the bay if we are to use Equation (15). This is inconvenient, as it is preferable to work in terms of conditions which arise at the hinge zone, such as the total mass input of the feeding glacier and the depth of bedrock where the glacier becomes afloat. We can however use these quantities if we consider the overall mass balance of the ice shelf. Let the volume input of the feeding glacier be $M$ (in units of $m^3 s^{-1}$ of ice at average density $\bar{\rho}$), and let the net accumulation $(a-m)$ be uniform over the entire area $2\lambda L$ of the ice shelf. Then, to balance input and output we must have

$$M + 2\lambda L(a-m)\rho_1/\bar{\rho} = 2\lambda H(X)u(X). \qquad (17)$$

Once reasonable values for volume input and net accumulation have been selected we can obtain a value for the product $H(X)u(X)$. There is then just one degree of freedom in our choice of boundary conditions; choosing $H(X)$ determines $u(X)$.

We can use this last degree of freedom to make a choice of $H(X)$ that will lead to an appropriate thickness of ice at the hinge zone, i.e. that thickness which will be just beginning to float when resting on the bedrock which is present at the hinge zone. The depth of bedrock at the hinge zone is thus the last remaining parameter we need to make the model determinate. For simplicity we shall consider the hinge zone to be in the form of an abrupt vertical edge at distance $L$ from the seaward margin of the bay, submerged at a depth $D$ below sea-level. We shall not consider here the possibility of instabilities in the position of the hinge zone (Weertman, 1974; Thomas and Bentley, 1978); such instabilities depend on the dynamics of the feeding glacier and on the slope of the bedrock, and are beyond the scope of this paper.

(ii) *Behaviour of the model*

It is found, when computing models of ice shelves, that the thickness calculated at the hinge zone is extremely sensitive to the values chosen for $H(X)$ and $u(X)$ at the seaward margin, but that, by making fine adjustments, the hinge-zone conditions can be exactly satisfied. It may seem unreasonable that an adjustment of a fraction of a metre in the value taken for $H(X)$ can lead to differences of 100 m and more in the value the model gives for thickness at the hinge zone. However, this peculiarity is only a result of the process of working backwards from the seaward margin, and does not reflect a physical instability. Quite the contrary, it merely means that large changes in the thickness and velocity at the hinge zone lead to relatively small changes at the seaward margin, provided that the total volume input is not altered. This is a physically reasonable result.

We shall look at the profile of an ice shelf in a bay 100 km wide and 150 km in length. We shall take the volume input to be $1.2 \times 10^{10}$ m³ a⁻¹, which corresponds, for instance, to an ice

shelf 600 m thick moving at 200 m $a^{-1}$ at the hinge zone. For flow and shear stress parameters we shall adopt the values found by Thomas (1973[a]) in his analysis of data from Amery Ice Shelf (Budd, 1966). He found that

$$\bar{B} = 1.39 \times 10^8 \text{ N m}^{-2} \text{ s}^{\frac{1}{3}} \qquad \text{and} \qquad \bar{\tau}_\text{s} = -9 \times 10^4 \text{ N m}^{-2}, \tag{18}$$

and we shall use the values

$$d = 0.467 \text{ Mg m}^{-3} \qquad \text{and} \qquad \bar{\rho} = 0.850 \text{ Mg m}^{-3}. \tag{19}$$

Three cases will be considered: an ice shelf undergoing zero net accumulation, one undergoing net accumulation of 0.5 m $a^{-1}$, and one undergoing net melting of 0.5 m $a^{-1}$. The model need make no distinction between the mass-balance contributions of snow-fall or ablation at the surface and freezing or melting at the bottom.
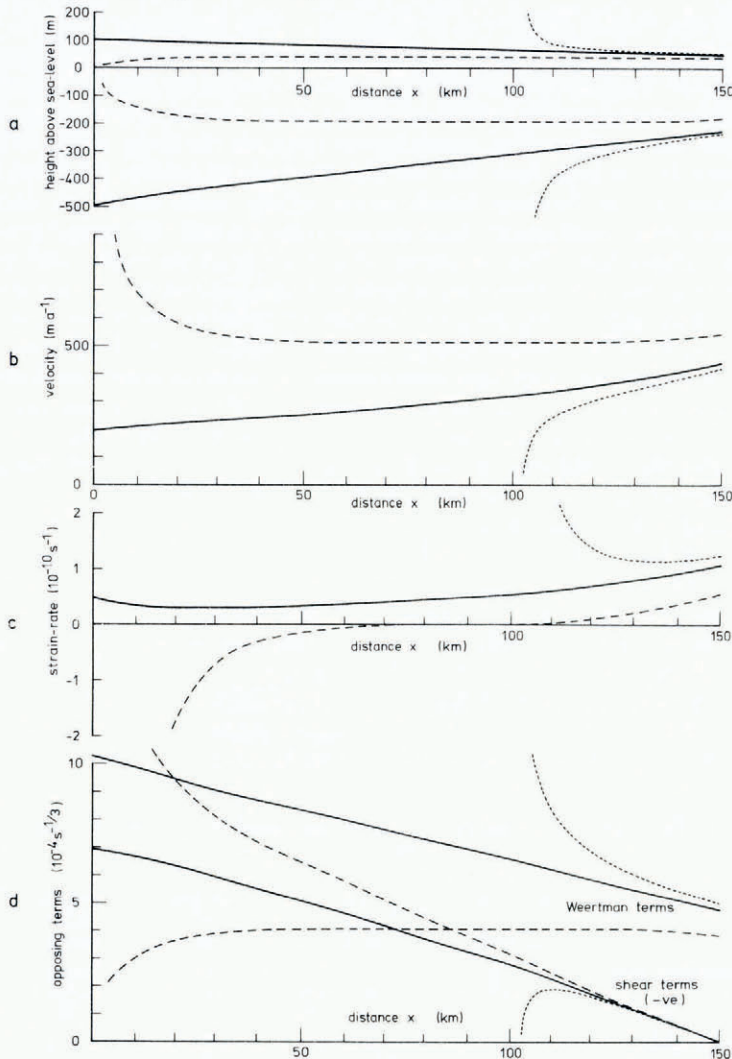


Fig. 5. *Behaviour of ice-shelf models for a parallel-sided bay with zero net accumulation: (a) ice thicknesses, (b) velocities, (c) strain-rates, and (d) the opposing terms, the Weertman term, and the shear term. The shear term is plotted as a positive quantity. The shorter dashes show the behaviour of a model with too great an initial thickness, the longer dashes one with too small an initial thickness.*

Figure 5 is intended to illustrate the general behaviour of the models. The essential feature of a bay ice shelf is the delicate balance between the driving force of weight of ice above sea-level and the restraining force due to shear at the bay sides. These two forces are represented by the two opposing terms in Equation (16):

$$\frac{gH}{2\bar{B}}\left\{\frac{(\rho_i-\bar{\rho})^2}{d}-\frac{\rho_i}{2}+\bar{\rho}-\frac{\bar{\rho}^2}{2\rho_w}\right\}, \tag{20}$$

which we shall call the "Weertman term", and

$$\frac{\bar{\tau}_s}{2\bar{B}H}\int_x^X\frac{H}{\lambda}\,dx, \tag{21}$$

which we shall call the "shear term" ($\bar{\tau}_s$ is negative). The choice we make in the initial conditions $H(X)$ and $u(X)$ is critical in any determination of which term dominates. If we start the model with too large a thickness at the seaward margin we find that the Weertman term dominates and increases rapidly; the ice shelf has large increasing extending strain-rates which result in rapid thickening as the model moves towards the hinge zone. If the chosen initial thickness is much too large then the ice shelf diverges to infinite thickness before the hinge zone is reached. If, on the other hand, we choose too small an initial thickness then the shear term dominates; strain-rates decrease inwards towards the hinge zone and can eventually become compressive. The thickness of the ice shelf decreases and may vanish before the hinge zone is reached. There are solutions of this kind which do not vanish before the hinge zone, but they give a very thin, fast-moving ice shelf at the hinge zone, and compressive strain over much of the ice-shelf length. We shall ignore these solutions as unrealistic, since most known ice shelves are thick and slow-moving at the hinge zone. In order to model conditions which arise in practice, we vary conditions at the seaward margin within the conditions prescribed by the general mass-balance formulation of Equation (17) until the model gives an appropriate thickness at the hinge zone. We shall take this thickness to be 600 m, which corresponds to hinge-zone bedrock at a depth of 496 m.

Table I for a parallel-sided bay shows the values calculated for $H(x)u(X)$ using Equation (17), and the values of $H(X)$ and $u(X)$ which were found to satisfy the hinge-line condition. They are shown for three cases: net accumulation of 0.5 m a$^{-1}$, which might correspond to 0.2 m a$^{-1}$ surface accumulation and 0.3 m a$^{-1}$ bottom freezing; zero net accumulation, which corresponds to surface accumulation exactly balanced by bottom melting; and net ablation of 0.5 m a$^{-1}$, which might correspond to 0.2 m a$^{-1}$ surface accumulation and 0.7 m a$^{-1}$ bottom melting. The thickness profiles are shown in Figure 5 (zero accumulation) and Figure 6 (net melt and freeze), together with the velocity, strain-rate, and the Weertman and shear terms. As expected, an ice shelf subject to melting is thinner and slower at the ice front

TABLE I. THICKNESS AND VELOCITY AT THE SEAWARD MARGIN FOR BAY ICE-SHELF MODELS

| | Net accumulation $a-m$ m a$^{-1}$ | Output $H(X)u(X)$ m$^2$ a$^{-1}$ | Thickness $H(X)$ m | Velocity $u(X)$ m a$^{-1}$ |
|---|---|---|---|---|
| Parallel-sided bay | 0.5 | $2.01\times10^5$ | 323.8 | 620.4 |
| | 0.0 | $1.20\times10^5$ | 272.4 | 440.6 |
| | −0.5 | $0.39\times10^5$ | 141.6 | 276.0 |
| Diverging bay | 0.5 | $1.29\times10^5$ | 258.4 | 500.9 |
| | 0.0 | $6.65\times10^4$ | 187.4 | 355.0 |
| | −0.5 | $3.64\times10^3$ | 13.0 | 280.1 |
| Converging bay | 0.5 | $2.58\times10^5$ | 366.3 | 704.3 |
| | 0.0 | $1.63\times10^5$ | 319.5 | 509.3 |
| | −0.5 | $6.74\times10^4$ | 224.0 | 300.9 |

than an ice shelf subject to freezing. However, it is an interesting feature of the solutions that the thickness in all three cases appears to change approximately linearly as we move back from the ice front, at least for some 100 km. Furthermore, it appears that the thickness gradient is very nearly the same for the three cases, even though the conditions of thickness, velocity, and melt are radically different. Changes in thickness gradient occur almost entirely within the last 50 km before the hinge zone: in the model with melting we find large slopes at the hinge zone, while with freezing the ice shelf is almost flat. Near the ice front the thickness gradients supplied by the model are: freeze, $2.08 \times 10^{-3}$; zero accumulation, $2.06 \times 10^{-3}$; melt, $2.23 \times 10^{-3}$. These show a spread of only eight per cent, whereas thicknesses in the three cases differ by a factor of two, velocities by a factor of three and strain-rates by an order of magnitude.

This happens because, if we refer to the graphs of the shear term (Figs 5(d) and 6(d)), we see that in the first 100 km from the ice front this term has very nearly the same form for the three different cases. That is, the restraining force due to shear at the sides seems to be practically independent of the thickness of the ice shelf. This can be shown mathematically.
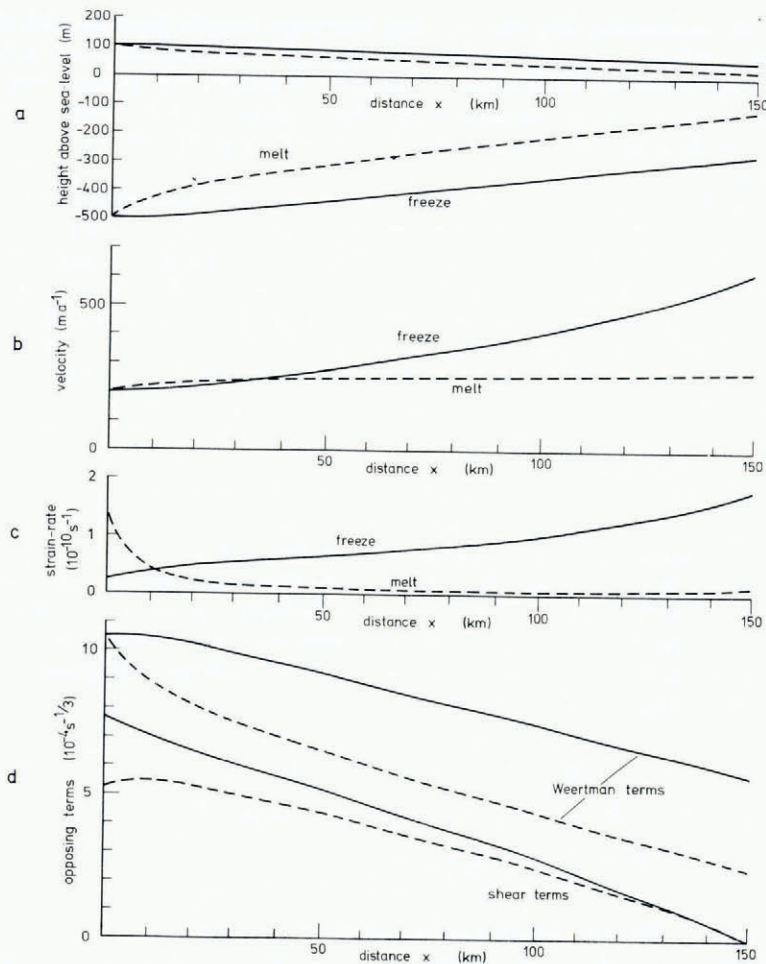


Fig. 6. *Behaviour of ice-shelf models for a parallel-sided bay with 0.5 m a⁻¹ melt (dashed line) and with 0.5 m a⁻¹ freezing (solid line).*

Consider an ice shelf of thickness $H(X)$ at the ice front with a small thickness gradient $\zeta$, so that thickness as a function of distance is

$$H(x) = H(X) + \zeta(X-x).$$

Then the shear term is given by

$$\frac{\bar{\tau}_s}{2\bar{B}H}\int_x^X \frac{H}{\lambda}\,dx = \frac{\bar{\tau}_s(X-x)}{2\bar{B}\lambda}\left[1+\frac{\zeta}{2H(X)}(X-x)\right]\left[1+\frac{\zeta}{H(X)}(X-x)\right]^{-1}.$$

Now $\frac{\zeta}{H(X)} \approx 10^{-5}$ m$^{-1}$, so $\frac{\zeta}{H(X)}(X-x)$ can be treated as a small quantity for distances within 50 km from the ice front and we can expand binomially to get

$$\frac{\bar{\tau}_s}{2\bar{B}H}\int_x^X \frac{H}{\lambda}\,dx \approx \frac{\bar{\tau}_s(X-x)}{2\bar{B}\lambda}\left[1-\frac{\zeta}{2H(X)}(X-x)\right].$$

This means that the restraining force due to shear increases roughly linearly with distance in from the ice front, and has a rate of increase of the order of, or slightly less than, $\bar{\tau}_s/2\bar{B}\lambda$. This quantity is clearly independent of thickness, velocity, or melt-rate. Our parameters give it the value of $6.47 \times 10^{-9}$ s$^{-\frac{1}{3}}$ m$^{-1}$ which compares with values from our models of: freeze, $6.21 \times 10^{-9}$ s$^{-\frac{1}{3}}$ m$^{-1}$; zero accumulation, $6.18 \times 10^{-9}$ s$^{-\frac{1}{3}}$ m$^{-1}$; and melt, $5.98 \times 10^{-9}$ s$^{-\frac{1}{3}}$ m$^{-1}$. This agreement is satisfactory.

Let us see what this means for the dynamics of a stable ice shelf. Shear force increases steadily, and almost linearly, as we move inwards from the ice front and has to be counterbalanced by the driving force due to the weight of ice above sea-level. It may be seen from the graphs of these two opposing forces that in order for a large stable ice shelf to exist they must just keep pace with each other. If the Weertman term begins to dominate then the ice shelf diverges to infinite thickness before the hinge zone; if the shear force dominates the ice shelf converges and vanishes. The difference between the two forces must remain approximately constant. Thus, in the three models we find that the Weertman term has quite different absolute values and yet approximately the same rate of increase with distance. In our models the Weertman term increases at the following rates: freeze, $3.70 \times 10^{-9}$ s$^{-\frac{1}{3}}$ m$^{-1}$; zero accumulation, $3.66 \times 10^{-9}$ s$^{-\frac{1}{3}}$ m$^{-1}$; and melt, $3.84 \times 10^{-9}$ s$^{-\frac{1}{3}}$ m$^{-1}$. These are some 40% less than the rates of increase of the shear parameter given above, a feature which is reflected in the fact that the strain-rate (which is given by the cube of the difference of the two quantities) decreases as we travel inland. Nonetheless, the quantities are nearly enough equal that we can use this as the basis for a calculation of an expected value for the ice-shelf gradient.

Let us assert that the rates of increase of the Weertman term (Equation (20)) and the shear term (Equation (21)) must be approximately equal for a large, stable ice shelf to exist. The rate of increase of the Weertman term is

$$\frac{g}{2\bar{B}}\left[\frac{(\rho_i-\bar{\rho})^2}{d}-\frac{\rho_i}{2}+\bar{\rho}-\frac{\bar{\rho}^2}{2\rho_w}\right]\frac{\partial H}{\partial x},$$

and the rate of increase of the shear term is $\bar{\tau}_s/2\bar{B}\lambda$. Equating these leads to

$$\frac{\partial H}{\partial x} = \bar{\tau}_s \bigg/ \left[g\lambda\left\{\frac{(\rho_i-\bar{\rho})^2}{d}-\frac{\rho_i}{2}+\bar{\rho}-\frac{\bar{\rho}^2}{2\rho_w}\right\}\right]. \tag{22}$$

This gives the expected thickness gradient of an ice shelf in terms of its density, its half-width, and the shear stress at the sides. In this approximation the thickness gradient is independent of melt or accumulation, flow-law parameters, thickness, and velocity. We only expect the formula to be approximate as we have equated two quantities which, in our modelled cases,

differ by 40%; indeed, Equation (22) predicts a thickness gradient of $3.7 \times 10^{-3}$ for an ice shelf with the parameters used in our models, which is greater than the modelled values by 75%. We should therefore trust the formula only to within a factor of about two.

(iii) *Agreement with reality*

The important feature of Equation (22) is its inverse dependence on half-width. The factor

$$\left\{ g \left[ \frac{(\rho_i - \bar{\rho})^2}{d} - \frac{\rho_i}{2} + \bar{\rho} - \frac{\bar{\rho}^2}{2\rho_w} \right] \right\}^{-1}$$

is approximately constant for different ice shelves and has a value of $1.85 \times 10^2$ m when the parameters of equalities (18) and (19) are used. Let us see how the rule agrees with available data. Figure 7 shows thickness gradient plotted against half-width for various bay ice shelves. The error bars shown for each set of data do not represent the experimental errors made in determining the quantities shown, they represent the range of values typically found for the quantities on each ice shelf. Thickness gradients have been taken for the middle region of the ice shelves, well away from the bay walls, the hinge zone, and the ice front, and the Ross Ice Shelf has been considered to be a single ice shelf, even though it is dominated by major ice streams (Robin, 1975). These streams give rise to a large scatter in the thickness gradients. The solid line in the graph shows the theoretical curve based on Equation (22), the agreement is satisfactory, both in form and in magnitude. The curve has been drawn using the data of equalities (18) and (19), yet it coincides almost exactly with a hyperbola fitted by regression.
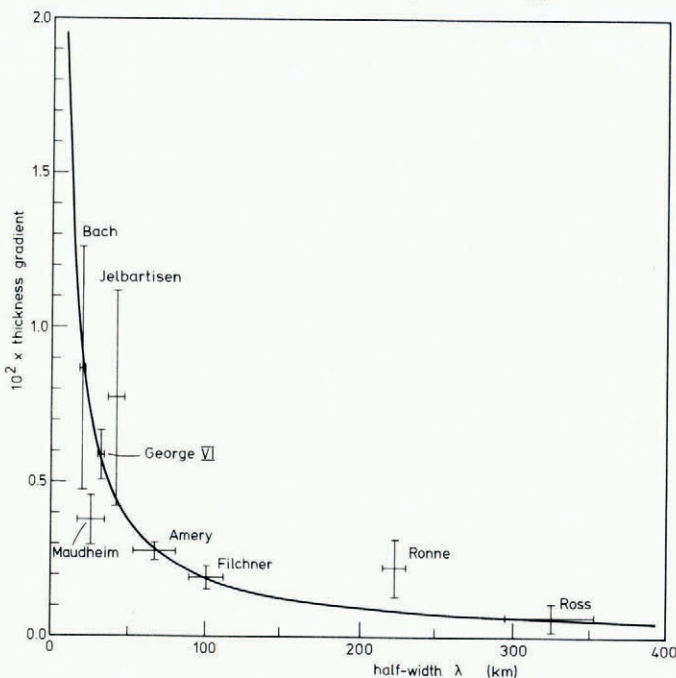


Fig. 7. *Relationship between thickness gradient and half-width for ice shelves. The solid line shows the theoretical curve based on Equation (22). Data are plotted for eight ice shelves: Bach Ice Shelf (J. F. Bishop, personal communication); Jelbartisen (Autenboer and Decleir, 1975); George VI Ice Shelf, southern end (J. F. Bishop, personal communication); Maudheim Is-shelf (Swithinbank, 1957); Amery Ice Shelf (Thomas, 1973[a]); Filchner Ice Shelf (Scott Polar Research Institute radio-echo flights); Ronne Ice Shelf (Swithinbank, 1977); and Ross Ice Shelf (Robin, 1975). The bars show the range of values typically found on each ice shelf.*

The slightly anomalous results for the Maudheim, Jelbartisen, and Ronne ice shelves can be explained in a number of ways: a different mean temperature through the ice shelf would very likely lead to a different value for the limiting shear $\bar{\tau}_s$ at the sides; different density parameters would alter the density term in the solution; and, more importantly, not all the ice shelves lie in bays which have almost parallel sides. Maudheim Is-shelf clearly converges while the Jelbartisen, and indeed the Amery Ice Shelf, diverge. Nevertheless, all the ice shelves studied show behaviour which lies within a factor of two of that predicted.

## IV. BAY ICE SHELVES WITH DIVERGING SIDES

### (i) *Theory*

Consider now an ice shelf which has formed in a bay with diverging, though still vertical, bay walls. Each wall diverges at an angle $\psi$ (Fig. 4b). The ice shelf now widens as it flows out to sea since it is no longer restrained in the $y$ direction. If the divergence of the bay is sufficiently gentle, then the ice shelf will spread sufficiently rapidly in the transverse direction to fill the entire width of the bay. This means that, for an ice shelf moving forward with an average velocity $\bar{u}$, the average strain-rate over width in the $y$ direction must be

$$\bar{\dot{\epsilon}} = \frac{\bar{u}}{\lambda} \tan \psi. \tag{23}$$

Budd (1966, p. 352) shows theoretically that, with the flow parameter $n = 3$, shear strain is concentrated towards the sides of an ice shelf; the effect is observed to be even more pronounced (Swithinbank, 1963; Hughes, 1977). Velocity changes little over the width of the shelf, so the average velocity is close to that of the centre line. Here I shall consider the average velocity to be equal to that calculated for the centre line. The mass-balance equation (4) then becomes:

$$\frac{\rho_1(a-m)}{\bar{\rho}} - H\left(\dot{\epsilon}_{xx} + \frac{u}{\lambda}\tan\psi\right) - u\frac{\partial H}{\partial x} = 0. \tag{24}$$

A more precise definition of "sufficiently gentle divergence" can be given by looking at the maximum possible rate at which an ice shelf can creep in the transverse direction. For a given thickness of ice shelf this maximum rate occurs for an unconfined glacier tongue, and is, by Equation (9),

$$\dot{\epsilon}_{yy} = \frac{1}{\sqrt{3}}\left[\frac{g}{\bar{B}\sqrt{3}}\left\{\frac{(\bar{\rho}-\rho_1)^2}{d} + \bar{\rho} - \frac{\rho_1}{2} - \frac{\bar{\rho}^2}{2\rho_w}\right\}\right]^n H^n. \tag{25}$$

The maximum permissible divergence of the ice shelf sides $\psi_{max}$ is then given by combining Equations (23) and (25) to give

$$\tan\psi_{max} = \frac{\lambda}{u\sqrt{3}}\left[\frac{g}{\bar{B}\sqrt{3}}\left\{\frac{(\bar{\rho}-\rho_1)^2}{d} + \bar{\rho} - \frac{\rho_1}{2} - \frac{\bar{\rho}^2}{2\rho_w}\right\}\right]^n H^n.$$

The substitution of values from equalities (18) and (19) indicates that

$$\tan\psi_{max} = 4.795 \times 10^{-18}\frac{\lambda H^n}{u}. \tag{26}$$

This equation shows that as an ice shelf flows in a diverging bay, becoming both faster and thinner towards the front, there will come a point where the ice shelf is unable to sustain sufficient transverse creep for it to remain intact. It should then either come adrift from the bay sides or develop crevasses and areas of weakness. It is then likely to break up. The most important factor in Equation (26) is the thickness term. The thickness of an ice shelf typically varies by a factor of about three between the hinge zone and the ice front so that $H^3$ is expected

to vary by a factor of about 30. The velocity and the half-width vary by factors of only two or three, and both increase towards the ice front, so that their ratio remains relatively stable. For an ice shelf of half-width 50 km and velocity 300 m a$^{-1}$ we can therefore write

$$\tan \psi_{max} \approx 2.52 \times 10^{-8} H^n,$$

which yields the critical thickness at which a typical ice shelf must come adrift from bay walls of a certain angle of divergence $\psi$. Table II shows the relationship. If an ice shelf of these assumed dimensions exists in a bay with sides diverging at 10° or 20° we expect it to become free from the sides once it has thinned to a thickness of 200–250 m. This might explain why the Amery Ice Shelf, for instance, extends no further than it does in its diverging bay; at the front its thickness is 270 m (Thomas, 1973[a]), its velocity is about 1 250 m a$^{-1}$ (Budd, 1966) and the half-width is about 100 km. According to Equation (26) this means that the maximum permissible divergence before the ice shelf comes adrift is $\psi_{max} = 13.4°$. The actual divergence at the front is about 16°, increasing to 26° (angles taken from the plan view in Thomas (1973[a], p. 63)).

TABLE II. MAXIMUM ANGLE OF DIVERGENCE $\psi_{max}$ OF A BAY BEFORE THE ICE SHELF COMES ADRIFT FROM THE SIDES, FOR AN ICE SHELF OF HALF-WIDTH 50 km, VELOCITY 300 m a$^{-1}$, AND THICKNESS $H$

| $H$ m | $\psi_{max}$ deg |
|---|---|
| 100 | 1.4 |
| 150 | 4.9 |
| 200 | 11.4 |
| 250 | 21.0 |
| 300 | 34.2 |
| 350 | 47.2 |
| 400 | 58.2 |

In order to derive an expression for the equilibrium profile of an ice shelf in a diverging bay we now need to use Equation (24) with a suitable expression for $\dot{\epsilon}_{xx}$; Equation (12) gives the general form of this expression. In order to use it we need to know a value for $\alpha$ in Equation (13), which expresses the effect of transverse stress deviators on the flow law; $\alpha$ is defined by $\dot{\epsilon}_{yy} = \alpha \dot{\epsilon}_{xx}$, and is therefore important only when the transverse strain-rate becomes comparable with the strain-rate in the $x$ direction. For $n = 3$, we find that $\alpha = 1$ gives $\theta = 0.111$, $\alpha = \frac{1}{2}$ gives $\theta = 0.112$, and $\alpha = 0$ gives $\theta = 0.125$. For most of the ice shelf we shall find that $\dot{\epsilon}_{yy} \ll \dot{\epsilon}_{xx}$, so that if we take $\theta = 0.125$, as in Equation (14), we shall be risking errors of at most ten per cent.

An exact treatment is much more complicated and not worthwhile since other parameters, such as $m$ and $\bar{B}$, are not known to better than ten per cent. In what follows we shall therefore use Equation (14) as before with one minor modification: because flow lines are diverging and, at the edges of the ice shelf, parallel to the bay walls, the shear stress $\bar{\tau}_s$ no longer acts in the same direction as the centre line of the ice shelf. Along the centre line the component of shear drag is $\bar{\tau}_s \cos \psi$ which, for small angles, leads to very little change. For the equilibrium profile we therefore have:

$$\frac{\partial H}{\partial x} = \left\{ \frac{\rho_i(a-m)}{\bar{\rho}} - H\left(\dot{\epsilon}_{xx} + \frac{u}{\lambda}\tan\psi\right) \right\} \bigg/ \left\{ u(X) + \int_x^x \dot{\epsilon}_{xx}\, dx \right\},$$

where

$$\dot{\epsilon}_{xx} = \left[\frac{gH}{2\bar{B}}\left\{\frac{(\rho_i-\bar{\rho})^2}{d} - \frac{\rho_i}{2} + \bar{\rho} - \frac{\bar{\rho}^2}{2\rho_w}\right\} + \frac{\bar{\tau}_s}{2\bar{B}H}\cos\psi \int_x^X \frac{H}{\lambda}\,\mathrm{d}x\right]^n. \qquad (27)$$

The quantity $\lambda$ in the shear integral is now a variable with the form

$$\lambda(x) = \lambda(0) + x\tan\psi,$$

where $\lambda(0)$ is the half-width of the ice shelf at the hinge zone.

### (iii) *Behaviour of the model*

We retain the input conditions of our previous model, a volume input of $1.2\times10^{10}$ m³ a⁻¹ over a hinge zone which is 100 km wide with ice 600 m deep. We retain the values previously used for $\bar{\tau}_s$, $\bar{B}$, $\bar{\rho}$, and $d$, but we now have a divergence angle $\psi$ of 15°. At the front the bay walls are therefore 180.4 km apart. Our equation for general mass balance becomes

$$M + \frac{\rho_i(a-m)}{\bar{\rho}}\,X[\lambda(0)+X\tan\psi] = 2H(X)u(X)[\lambda(0)+X\tan\psi].$$

Table I shows values of $H(X)u(X)$ calculated for a diverging bay using this equation and the values of $H(X)$ and $u(X)$ which satisfy the hinge-line conditions, for the three cases of net freezing, zero net accumulation, and net melting. We can, using Equation (26), calculate the maximum permissible bay divergence for these three models if the ice shelf is to remain intact, it is 25° for net freezing, 14° for zero net accumulation, and 0.01° for net melting. Since the actual bay divergence is 15° this means that with net freezing the ice shelf is stable, with zero net accumulation it just becomes unstable as it nears the seaward margin, and with net melting it is quite unstable and the ice shelf would come adrift long before reaching the seaward margin of the bay. The model treatment is therefore not valid in this case, since it assumes contact with the bay walls over the entire length of the bay.

We conclude that an ice shelf which is undergoing melt cannot exist in the entire length of the bay for the assumed input conditions. A smaller ice shelf can form, but it terminates before the seaward margin of the bay is reached. By a lengthy process of trial and error we find that an ice shelf extending 38 km from the hinge zone can form and remain in contact
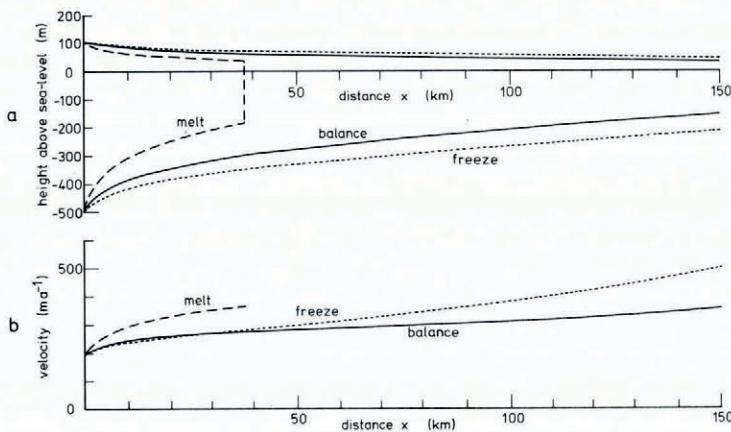


Fig. 8. Behaviour of ice-shelf models in a bay with sides diverging at 15°, for 0.5 m a⁻¹ melt (longer dashes); net balance of melt and accumulation (solid line); and 0.5 m a⁻¹ freezing (shorter dashes). The melting ice shelf can extend 38 km before it comes adrift from the bay walls.

with the bay walls. At the 38 km point it has a thickness of 220.7 m and a velocity of 366.8 m a$^{-1}$, for which the critical bay divergence is 15°. With further thinning, the ice shelf can no longer cope with the divergence of the bay and so comes adrift. The form of the solution is shown in Figure 8.

## V. Bay ice shelves with converging sides

We now consider an ice shelf which has formed in a bay with converging sides (Fig. 4c). In an extreme case, where the sides converge quite rapidly, the ice shelf will flow very much faster and even perhaps become thicker as it moves through the narrowing bay. This will lead to preferential erosion of the narrower parts of the bay, with the result that the sides of the bay should tend eventually to become parallel. This could account for the observed fact that there are few ice shelves in existence which can properly be described as converging. We shall take the angle of convergence to be five degrees. The analysis for the diverging case still applies (p. 452), but with the angle $\psi$ now negative, and without any conditions necessary on the maximum allowable transverse strain-rate which is now compressive. We retain the input conditions of previous models. At the seaward margin the bay is 73.8 km wide.

Table I for a converging bay shows the results of model calculations, and the form of the solutions is shown in Figure 9. It is seen that in a converging bay the model allows the ice shelf initially to become thicker as we move away from the hinge zone. This is especially noticeable for the case of net freezing, but occurs also for the case of zero net accumulation.
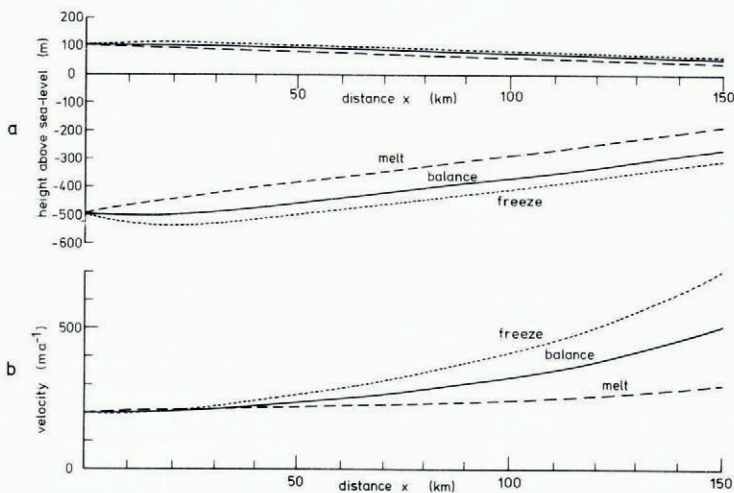


Fig. 9. *Behaviour of ice-shelf models in a bay with sides converging at 5°, for 0.5 m a$^{-1}$ melt (longer dashes); net balance (solid line); and 0.5 m a$^{-1}$ freezing (shorter dashes).*

## VI. Effect of pinning by ice rises and areas of grounding

Swithinbank (1957, p. 34) suggests that areas of grounding towards the seaward margin of an ice shelf are very important to its stability and concludes that "an ice shelf, unless it is flanked by land or by inland ice sheets, will never extend far to sea beyond the outermost shoals which could ground it". This rule has been found to be generally true even to the extent that, where an unconfined ice shelf appears from maps to extend well beyond known areas of grounding, it has proved fruitful to look more closely for unnoticed areas of grounding towards the ice front. In the case of ice shelves which are pinned by grounding areas out to sea, but are not flanked by land or inland ice sheets, the increased stability is largely due to

increased resistance to the destructive action of tides and tsunamis. It is not due to any effect of the pinning on the overall form of the ice shelf; the presence of grounding areas will have some effect on the thickness profile of the ice shelf, but very little, since the ice shelf is still free to thin in the transverse direction. However, for a bay ice shelf we find, as Thomas (1976) proposes, that the presence of pinning ice rises and grounding areas towards the mouth of the bay can radically alter the thickness profile. They provide an appreciable up-stream restraining force, preventing the ice shelf from thinning as rapidly as it would if it were not pinned. Thinning in the transverse direction is of course controlled by the divergence of the bay.
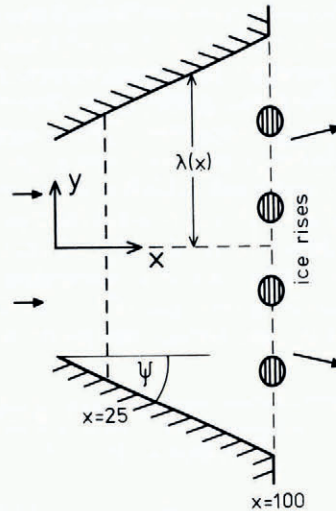


Fig. 10. Plan view of an ice shelf in a bay diverging at 25° with pinning ice rises towards the ice front. Without pinning ice rises the ice shelf can remain in contact with the bay walls only until the 25 km mark, with pinning it can fill the entire bay.

To illustrate this we shall consider a bay diverging quite widely, with $\psi = 25°$, and undergoing zero net accumulation. We shall take it to be 100 km wide at the hinge zone and to extend for 100 km (Fig. 10). It is therefore 193.3 km wide at the seaward margin. We retain the input conditions of previous models. When we try to find an equilibrium ice shelf for this bay we encounter the same problem as in Section IV (p. 452): the ice shelf becomes so thin that it cannot sustain enough transverse creep to remain in contact with the walls of the bay. We find that it will last only 25 km before coming adrift from the sides, and at this point has thickness 264.9 m and velocity 367.3 m a$^{-1}$, this solution is shown in Figure 11.

Now we allow the ice shelf to become grounded towards the mouth of the bay. Following Thomas (1973[a]), we express the up-stream force due to grounding as a force per unit width of ice shelf acting along the entire length of the ice shelf. This means that at any point on the ice shelf the driving force of the weight of the ice above sea-level must overcome the sum of two forces opposing it: the force due to shear at the bay sides and the force due to restraint by grounding at the mouth of the bay. It is not clear whether the force due to grounding should be transmitted up-stream as a constant total force or as a constant force per unit width of ice shelf; for a diverging bay the two cases are distinct. In the first case the effect of the pinning becomes concentrated as we approach the narrower hinge zone, whereas in the second case its effect per unit width remains constant and part of the pinning force is balanced by forces at the sides. The answer to the question depends on whether we consider the ice shelf to behave as a rigid body or as a quasi-hydrostatic fluid. Ice behaviour is somewhere between these two
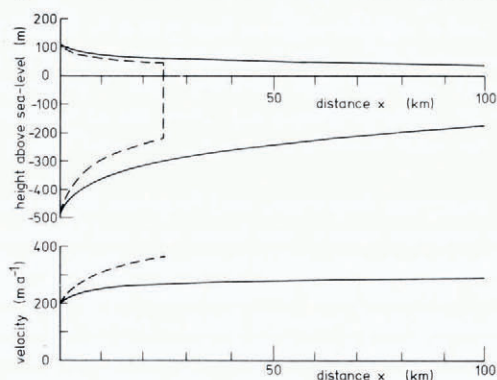
Fig. 11. *Behaviour of ice-shelf models in a bay with sides diverging at 25°, for zero net accumulation. The dashed line shows the extent of the ice shelf if no pinning ice rises are present. The solid line shows the ice shelf when ice rises are present towards the ice front.*

limits, but we shall assume constant force per unit width. This gives a lower limit for the effect of the pinning. The force due to grounding may be written as a force per unit width $F_g$, which modifies Equation (27) to

$$\dot{\epsilon}_{xx} = \left[\frac{gH}{2\bar{B}}\left\{\frac{(\rho_i - \bar{\rho})^2}{d} - \frac{\rho_i}{2} + \bar{\rho} - \frac{\bar{\rho}^2}{2\rho_w}\right\} + \frac{1}{2\bar{B}H}\left\{\bar{\tau}_s \cos\psi \int_x^X \frac{H}{\lambda}\,\mathrm{d}x - F_g\right\}\right]^n.$$

There is a wide choice of values we might take for $F_g$ depending on the nature and extent of grounding, there are two types of grounding we might consider: First, an ice shelf can become grounded over a single area large enough that conditions are favourable for the formation of an ice rise; such ice rises are miniature ice caps with a flow regime independent of the surrounding ice shelf and they are fed by accumulation at their surface. The ice shelf cannot flow over them and so has to flow round them. In doing so it undergoes large compressive stresses immediately up-stream of the ice rise and undergoes shear at the sides of the ice rise. If the ice shelf is of thickness $H$ and the ice rise has length $L$ and width $W$ we expect the total up-stream force to be approximately $H(2L\bar{\tau}_s + W\sigma_c)$ where $\bar{\tau}_s$ is the limiting shear stress and $\sigma_c$ is the limiting compressive stress. As in the case of shear at the sides of the bay we expect $\bar{\tau}_s$ to lie in the range 0.4–1.0 bar, depending on the strength of coupling between ice and rock. $\sigma_c$ is also likely to be of the order of one bar, though field measurements up-stream of ice rises have shown that it may reach three bars or more (personal communication from R. H. Thomas). For convenience we shall take both limiting stresses to be 0.9 bar, as before. Secondly, we consider smaller areas of grounding which are insufficient to stop the flow of the ice shelf completely. The ice shelf tries to flow over them and undergoes shear stress at the base. The disturbance results in surface undulations but not in the creation of an independent dynamic system. The total area $A$ of grounded ice multiplied by the stress limit gives the up-stream force $A\bar{\tau}_s$. (This is the model used by Thomas (1973[b]) to model the influence of the McDonald Ice Rumples on the Brunt Ice Shelf.)

A value of $2.4 \times 10^{12}$ N has been chosen for the total force exerted by grounding areas and ice rises at the seaward margin of the bay, which is equivalent to $12.5 \times 10^6$ N m⁻¹ over the width of the ice shelf. If $9 \times 10^4$ N m⁻² is the maximum stress sustainable by ice then this force represents $2.7 \times 10^7$ m² of ice at yield stress. This is equivalent to four ice rises of effective perimeter $(2L + W) = 30$ km, with surrounding ice shelf some 225 m thick, or to a total of 27 km² of grounding areas contributing basal drag. This extra restraining force, when applied to the ice-shelf model, gives a very different picture. At the seaward margin it now has

thickness $H(X) = 213.7$ m and a velocity $u(X) = 290.5$ m a$^{-1}$. These values supply (Equation (26)) a critical bay divergence of $26°$. The ice shelf is stable in a bay diverging at $25°$. The presence of grounding areas and ice rises therefore has a profound effect on the overall equilibrium of a bay ice shelf; without grounding areas the ice shelf is a minor one, extending only 25 km into the bay, but with them it is a major ice shelf which extends the full 100 km of the bay.

If a major ice shelf as described does exist, and depends for its existence on pinning at its seaward margin, we must enquire how it can have reached its grounding areas in the first place. As the model stands there are two stable states and there are several possibilities for the transition between the two. It could have resulted from congestion by build-up of grounded icebergs and sea ice, or it could have resulted from a period of more intense glacierization when the ice shelf was under different conditions of mass balance and perhaps extended well beyond the mouth of the bay. It would require only small changes in net accumulation to achieve this. It would occur for our model if, for instance, the climate during an ice age changed sufficiently that one metre per year of snow accumulation occurred at the upper surface of the ice shelf or, equivalently, one metre per year of freezing occurred at the lower surface. Another possibility is that climatic cooling might lead to a significant increase in the flow-law parameter $B$, leading to reduced thinning rates and to a thicker and slower ice shelf. It is interesting to note that the model ice shelf cannot be made stable by increasing hinge-zone input: if, for instance, we model an 800 m thick ice shelf moving at 500 m a$^{-1}$ at the hinge zone, we find a thickness of 216 m and a velocity of 957 m a$^{-1}$ at the seaward margin and this is unstable by Equation (26).

Areas of grounding need not only occur near the seaward margin of the bay: the Amery and Ross Ice Shelves both have important areas of grounding in the main body of the ice shelf. The methods outlined in the present paper are readily applicable to the determination of equilibrium profiles with the presence of ice rises at any point in the ice shelf. We have not tried to obtain a profile for the Amery Ice Shelf, since the data available are too sparse and approximate to lead to a test of any significance. Bottom freezing-rates have been calculated on the assumption of steady state and therefore the use of them in calculating a steady-state profile would produce a circular argument, and only demonstrate self-consistency. More important, Budd (1966) concluded from his data that the ice shelf is not in steady state, and thus our present theory would be inappropriate.

## VII. EXTENSIONS TO THE THEORY

1. If the valley walls are sloping instead of vertical we should expect the shear-stress term (Equation (21)) to be greater, since a greater area of ice is in contact with rock. If the angle of slope of the walls is $\phi$ from the vertical the average shear stress over depth should be increased by a factor of $(\cos \phi)^{-1}$.

2. Many ice shelves are not of uniform thickness in the transverse direction (personal communication from C. W. M. Swithinbank). They are thinner at the edges than in the central region. This means that the shear term for the central region of the ice shelf is reduced by the ratio of thickness at the edges to thickness in the centre. This ratio might be about $80\%$.

3. The theory might be modified to cope with ice streams within ice shelves. Such ice streams are subject to considerable drag as they come into contact with slower-moving surrounding ice, and they show large transverse thickness gradients at their boundaries. As they proceed, shear gradually disappears and the thickness becomes more uniform (Robin, 1975). In order to apply our theory we need to know the way in which shear varies.

4. Because the method of computation is not analytic, but proceeds by steps, it is possible to incorporate variation of the parameters $\bar{\tau}_s$, $\bar{\rho}$, $d$, $\lambda$, $\psi$, and $\bar{B}$ as we move along the ice shelf. Provided that these parameters are only varying slowly with distance, we can calculate the

model equilibrium profile of an ice shelf under almost any constant conditions of input, bay shape, and climate.

5. Thomas (1976) has raised the possibility that areas of grounding in an ice shelf may appear and disappear in response to isostatic uplift and depression of seabed beneath an ice shelf. If isostatic response is much slower than the time taken for an ice shelf to reach equilibrium then the present theory might be used to describe the effect of such events.

6. Once an equilibrium profile has been obtained it should be easy to determine whether or not a particular ice shelf is in equilibrium. If it is not, then it may be possible to analyse conditions of non-steady state by applying perturbations to the mass balance. Such an analysis might follow the lines described in Paterson (1969, chapter 11), using our calculated equilibrium profiles as a "datum state". This may form the subject of a separate paper.

## REFERENCES

Autenboer, T. van, *and* Decleir, H. 1975. Jelbartisen-Trolltunga, Dronning Maud Land, Antarctica. Radio-glaciological survey. Data report. 1969 Belgian Antarctic expedition. *Belgium. Service Géologique de Belgique. Professional Paper* 1975, No. 1.

Barkov, N. I. 1970. Ravnovesnaya i minimal'naya tolshchina shel'fovykh lednikov Antarktidy [Equilibrium and minimal thickness of the ice shelves of Antarctica]. *Trudy Arkticheskogo i Antarkticheskogo Nauchno-Issledovatel'skogo Instituta*, Tom 294, p. 127–41.

Budd, W. F. 1966. The dynamics of the Amery Ice Shelf. *Journal of Glaciology*, Vol. 6, No. 45, p. 335–58.

Carslaw, H. S., *and* Jaeger, J. C. 1959. *Conduction of heat in solids. Second edition*. Oxford, Clarendon Press.

Hobbs, P. V. 1974. *Ice physics*. Oxford, Clarendon Press.

Holdsworth, G. 1974. Erebus Glacier tongue, McMurdo Sound, Antarctica. *Journal of Glaciology*, Vol. 13, No. 67, p. 27–35.

Holdsworth, G. 1977. Tidal interaction with ice shelves. *Annales de Géophysique*, Tom. 33, Fasc. 1–2, p. 133–46.

Hughes, T. J. 1975. The West Antarctic ice sheet: instability, disintegration, and initiation of ice ages. *Reviews of Geophysics and Space Physics*, Vol. 13, No. 4, p. 502–26.

Hughes, T. J. 1977. West Antarctic ice streams. *Reviews of Geophysics and Space Physics*, Vol. 15, No. 1, p. 1–46.

Nye, J. F. 1959. The motion of ice sheets and glaciers. *Journal of Glaciology*, Vol. 3, No. 26, p. 493–507.

Paterson, W. S. B. 1969. *The physics of glaciers*. Oxford, Pergamon Press. (The Commonwealth and International Library. Geophysics Division.)

Robin, G. de Q. 1955. Ice movement and temperature distribution in glaciers and ice sheets. *Journal of Glaciology*, Vol. 2, No. 18, p. 523–32.

Robin, G. de Q. 1958. Glaciology. III. Seismic work and related investigations. *Norwegian–British–Swedish Antarctic Expedition, 1949–52. Scientific Results*, Vol. 5.

Robin, G. de Q. 1975. Ice shelves and ice flow. *Nature*, Vol. 253, No. 5488, p. 168–72.

Robin, G. de Q., *and others*. 1970. Radio echo exploration of the Antarctic ice sheet, by G. de Q. Robin, C. W. M. Swithinbank, and B. M. E. Smith. [*Union Géodésique et Géophysique Internationale. Association Internationale d'Hydrologie Scientifique*.] [*International Council of Scientific Unions. Scientific Committee on Antarctic Research. International Association of Scientific Hydrology. Commission of Snow and Ice*.] International Symposium on Antarctic Glaciological Exploration (ISAGE), Hanover, New Hampshire, U.S.A., 3–7 September 1968, p. 97–115. [(Publication No. 86 [de l'Association Internationale d'Hydrologie Scientifique].)]

Sanderson, T. J. O., *and* Doake, C. S. M. 1979. Is vertical shear in an ice shelf negligible? *Journal of Glaciology*, Vol. 22, No. 87, p. 285–92.

Schytt, V. 1958. Glaciology. II. The inner structure of the ice shelf at Maudheim as shown by core drilling. *Norwegian–British–Swedish Antarctic Expedition, 1949–52. Scientific Results*, Vol. 4, C.

Stuart, A. W., *and* Bull, C. B. B. 1963. Glaciological observations on the Ross Ice Shelf near Scott Base, Antarctica. *Journal of Glaciology*, Vol. 4, No. 34, p. 399–414.

Swithinbank, C. W. M. 1957. Glaciology. I. The morphology of the ice shelves of western Dronning Maud Land. *Norwegian–British–Swedish Antarctic Expedition, 1949–52. Scientific Results*, Vol. 3, A.

Swithinbank, C. W. M. 1963. Ice movement of valley glaciers flowing into the Ross Ice Shelf, Antarctica. *Science*, Vol. 141, No. 3580, p. 523–24.

Swithinbank, C. W. M. 1977. Glaciological research in the Antarctic Peninsula. *Philosophical Transactions of the Royal Society of London*, Ser. B, Vol. 279, No. 963, p. 161–83.

Thomas, R. H. 1973[a]. The creep of ice shelves: interpretation of observed behaviour. *Journal of Glaciology*, Vol. 12, No. 64, p. 55–70.

Thomas, R. H. 1973[b]. The creep of ice shelves: theory. *Journal of Glaciology*, Vol. 12, No. 64, p. 45–53.

Thomas, R. H. 1976. Thickening of the Ross Ice Shelf and equilibrium state of the West Antarctic ice sheet. *Nature*, Vol. 259, No. 5540, p. 180–83.

Thomas, R. H., *and* Bentley, C. R. 1978. A model for Holocene retreat of the West Antarctic ice sheet. *Quaternary Research*, Vol. 10, No. 2, p. 150–70.

Weertman, J. 1957. Deformation of floating ice shelves. *Journal of Glaciology*, Vol. 3, No. 21, p. 38–42.

Weertman, J. 1974. Stability of the junction of an ice sheet and an ice shelf. *Journal of Glaciology*, Vol. 13, No. 67, p. 3–11.

Wexler, H. 1960. Heating and melting of floating ice shelves. *Journal of Glaciology*, Vol. 3, No. 27, p. 626–45.